

## Comparing Anisotropic Diffusion Filters: Enhancement of $^{23}\text{Na}$ MRI of Human Kidney

Frank G Zoellner<sup>1</sup>, Christoph M Decker<sup>1</sup>, Simon Konstandin<sup>1</sup>, and Lothar R Schad<sup>1</sup>

<sup>1</sup>Computer Assisted Clinical Medicine, Heidelberg University, Mannheim, Germany

### Introduction

In-vivo MR imaging of sodium is limited due to its electro-physiological characteristics. The combination of relative low in-vivo concentration and MR sensitivity of  $^{23}\text{Na}$  compared to  $^1\text{H}$  results in relative low in-vivo MR signal. Therefore, a logical step forward is to enhance image intensity by applying post-processing filters while Gibb's ringing could also be suppressed. Recently, Fermi filters were applied to  $^{23}\text{Na}$  MRI [1]. The increase in signal-to-noise ratio by linear filters as previously proposed is paid by a loss in resolution (blurring). Filters that preserve contours while removing noise are anisotropic diffusion filters (AND). AND model a diffusion process, smoothing areas with weak edges and preserving or enhancing strong edges in the image. The typical blurring of linear filters is reduced. AND was first applied to  $^1\text{H}$  MR images of the brain [2]. Initial results on AND filtering in  $^{23}\text{Na}$  MRI were recently reported [3]. The aim of this study was to compare different anisotropic filters for enhancing sodium MR images of the kidney.

Filter	Rel. $\sigma_b$	Rel. RSS
Original image	1	0
3D-AND ( $i=10$ , $\Delta t = 3/44$ , $K = 300$ )	$0.01 \pm 0.01$	2.7
2D-AND ( $i=10$ , $\Delta t = 1/7$ , $K = 300$ )	$0.05 \pm 0.04$	1.0
3D-AND iterative $K$ ( $i=10$ , $\Delta t = 3/44$ , $q = 0.6$ )	$0.01 \pm 0.02$	5.2
2D-AND iterative $K$ ( $i=10$ , $\Delta t = 1/7$ , $q = 0.7$ )	$0.04 \pm 0.03$	1.9
2D-AND hog $K$ ( $i=2$ , $\Delta t = 0.1$ , $h^t = 0.68$ , $h^T = 0.99$ )	$0.12 \pm 0.13$	167.9
2D-AND tensor ( $i=50$ , $\Delta t = 0.01$ , $K = 1$ , $\sigma = 1$ , $k = 3$ , $\rho = 1$ , $h = 3$ )	$0.17 \pm 0.15$	48.3

**Tab. 1:** Minimum  $\sigma_b$  and relative residual sum of squares for the six AND filters. Filter parameters are given in brackets ( $i$  = number of iterations,  $\Delta t$  = time step,  $K$  = threshold,  $q$  = quantile for Canny's noise estimator).

### Materials and Methods

Four data sets were acquired on a 3.0 T clinical whole-body MR scanner. For  $^{23}\text{Na}$ -signal reception a commercially-available dedicated  $^{23}\text{Na}$ -tuned cardiac coil with 8-coil elements was used. A density adapted three-dimensional gradient-echo sequence with radial trajectories was used for image acquisition [4] with TR/TE/FA = 120 ms / 0.55 ms / 85°, FOV = 320 x 320 mm<sup>2</sup>, readout length per spoke = 20 ms, projections = 8000 resulting in a TA = 16 min and a nominal isotropic spatial resolution of 5 mm. The diffusion coefficient  $c(x,y,t)$  depends on both time and space coordinates [5]:  $\partial I / \partial t = \nabla(c(x,y,t)\nabla I)$ . Ideally,  $c(x,y,t)$  is set to 0 at region boundaries and 1 otherwise – but as the correct region boundaries are yet unknown,  $c(x,y,t)$  is chosen as a function  $g(E)$  of the edge estimate  $E(x,y,t)$ , with a threshold  $\kappa$ , below which noise is smoothed and above which edges are enhanced. The simplest choice for  $E$  is the gradient image  $\nabla I(x,y,z,t)$ :  $g(E) = (1 + (|\nabla I|/\kappa)^2)^{-1}$ . Six different variants of AND filters were compared: 2D- and 3D-AND filter with/without (automatically) iteratively determined  $\kappa$ , a histogram of gradient (HOG) AND [6] where  $c(x,y,z,t)$  depends on the histogram frequencies of the intensity gradients, and an adapted diffusion tensor [7]. The optimal parameters of each method were determined by looking at the standard deviation  $\sigma_b$  in the background – and at the background noise level to avoid losing much of the signal intensity. To observe the filter properties in different intensity ranges, many different ROIs amidst the signal in all kidneys and data sets were selected and mean intensities were calculated for the filtered images and plotted against those of the original image to examine their correlation. In addition, the residual sums of squares (RSS) between the measured intensities and the original intensities were computed.

### Results

Sampling the whole parameter space ( $\kappa = \{100, \dots, 1000\}$  and  $N = \{1, \dots, 15\}$ ) revealed that at  $i = 5$  and  $\kappa = 300$  the noise is reduced by 80%. The minimum  $\sigma_b$  for a signal decrease of less than 5% and the RSS for the six different variants of the AND filter are given in Tab. 1. Figure 1 shows several slices of one volunteer comprising unfiltered, 2D- and 3D-AND filtered images. The corresponding characteristic lines are depicted in Fig. 2.

### Discussion

For HOG 2D-AND and tensor-based 2D-AND more than 30% of the signal is omitted. 2D-AND with/without iterative  $\kappa$  versions performed best, depicted by a close line to the angular bisector. The 3D-AND with/without iterative  $\kappa$  performs slightly worse than the 2D version, but the signal loss is below 5%. For comparison, a standard Gaussian filter has an identical behavior than the tensor-based AND – it fails at small structures with high gradients. It could be shown that the idea behind the concept of anisotropic diffusion filtering – smoothing within regions and along boundaries, but not across them – works satisfactory on low-resolution sodium MR images and can be successfully used to enhance them for further analyses. We envision that by using AND filters, quantitative analysis of the corticomedullary  $^{23}\text{Na}$  gradient could be improved.

### References

- [1] Maril N, et al., Magn Reson Med. 2006. 56(6), pp.1229-34
- [2] Gerig G, et al. IEEE Trans Med Imaging. 1992. 11(2), pp. 221-232
- [3] Decker CM, et al., ISPA 2011, pp. 762-766
- [4] Nagel AM, et al., Magn Reson Med. 2009. 62 (6), pp.1565-1573
- [5] Perona P, Malik J. IEEE Trans PAMI. 1990. 12(7), pp. 629-639
- [6] Bajla I, et al. Computer Analysis of Images and Patterns. 1993. pp. 90-97
- [7] Weickert J. Computing Supplements. 1996. 11, pp. 221-236

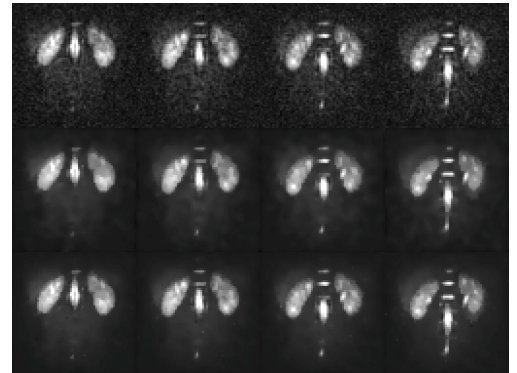


**Fig. 1:** Four central slices of sodium MR images of human kidney of volunteer 1. Upper row: unfiltered image, middle row: 2D AND filtered images, lower row: 3D AND filtered images.

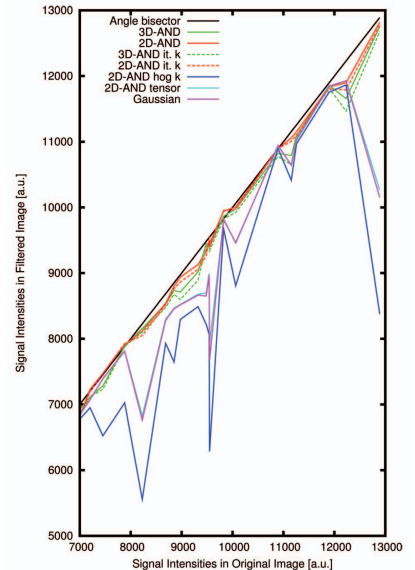


**Fig. 2:** Characteristic of the six different AND filters and the linear Gaussian filter.